Characterization of a Novel α1,2-Fucosyltransferase of *Escherichia coli* O128:B12 and Functional Investigation of Its Common Motif

Mei Li,[‡,§] Xian-Wei Liu,[‖,⊥] Jun Shao,[‡] Jie Shen,[‖] Qiang Jia,[‡] Wen Yi,[‖] Jing K. Song,[‖,⊥] Robert Woodward,[‖] Christine S. Chow,[‡] and Peng George Wang*,[‖]

Department of Chemistry, Wayne State University, Detroit, Michigan 48202, and Department of Biochemistry and Chemistry, The Ohio State University, Columbus, Ohio 43210

Received July 9, 2007; Revised Manuscript Received October 16, 2007

ABSTRACT: The *wbsJ* gene from *Escherichia coli* O128:B12 encodes an α1,2-fucosyltransferase responsible for adding a fucose onto the galactose residue of the O-antigen repeating unit via an α1,2 linkage. The *wbsJ* gene was overexpressed in *E. coli* BL21 (DE3) as a fusion protein with glutathione S-transferase (GST) at its N-terminus. GST-WbsJ fusion protein was purified to homogeneity via GST affinity chromatography followed by size exclusion chromatography. The enzyme showed broad acceptor specificity with Gal*β*1,3GalNAc (T antigen), Gal*β*1,4Man and Gal*β*1,4Glc (lactose) being better acceptors than Gal*β*-*O*-Me and galactose. Gal*β*1,4Fru (lactulose), a natural sugar, was furthermore found to be the best acceptor for GST-WbsJ with a reaction rate four times faster than that of lactose. Kinetic studies showed that GST-WbsJ has a higher affinity for lactose than lactulose with apparent K_m values of 7.81 mM and 13.26 mM, respectively. However, the $k_{cat}/^{app}K_m$ value of lactose (6.36 $M^{-1}\cdot min^{-1}$) is two times lower than that of lactulose (13.39 $M^{-1}\cdot min^{-1}$). In addition, the α1,2-fucosyltransferase activity of GST-WbsJ was found to be independent of divalent metal ions such as Mn^{2+} or Mg^{2+}. This activity was competitively inhibited by GDP with a K_i value of 1.41 mM. Site-directed mutagenesis and a GDP-bead binding assay were also performed to investigate the functions of the highly conserved motif $H^{152}xR^{154}R^{155}xD^{157}$. In contrast to α1,6-fucosyltransferases, none of the mutants of WbsJ within this motif exhibited a complete loss of enzyme activity. However, residues R^{154} and D^{157} were found to play critical roles in donor binding and enzyme activity. The results suggest that the common motif shared by both α1,2-fucosyltransferases and α1,6-fucosyltransferases have similar functions. Enzymatic synthesis of fucosylated sugars in milligram scale was successfully performed using Gal*β*-*O*-Me and Gal*β*1,4Glc*β*-N_3 as acceptors.

In mammals, L-fucose is an important residue in glycoconjugates, such as ABH and Lewis antigens, either bound to the cell membrane or secreted into biological fluids (*1*). These fucosylated carbohydrates are involved in a wide range of cellular processes such as cell adhesion, the inflammatory response, leucocyte trafficking and fertilization (*2*). In prokaryotes, L-fucose is mainly present in polysaccharides of the cell wall and has been suggested to be involved in mimicry, adhesion, localization and modulating the host immune response (*3*).

Fucosylations are accomplished by fucosyltransferases (FucTs[1]), which catalyze the transfer of fucose from GDP-*β*-L-fucose to various oligosaccharides or proteins. Based on the linkage type, FucTs are classified into four subfamilies: α1,2-FucTs, α1,3/4-FucTs, α1,6-FucTs and *O*-FucTs. α1,2-FucTs and α1,6-FucTs are evolutionary closely related subfamilies, sharing three motifs in their catalytic C-terminal domains (*4*). α1,2-FucTs belong to glycosyltransferase family 11 (http://www.cazy.org/fam/acc_GT.html), catalyzing an inversion reaction by transfer of fucose from GDP-*β*-L-fucose to a galactose (Gal) residue to form an α1,2-linkage. α1,6-FucTs, however, are categorized into glycosyltransferase family 23, transferring fucose from GDP-*β*-L-fucose to a *N*-acetylglucosamine (GlcNAc) residue to form an α1,6-linkage (*5*). To date, many of the genes encoding α1,2-FucTs have been cloned from humans (*6*−*9*), various animal species (*10*, *11*), invertebrates (*12*) and plants (*13*). In humans, α1,2-FucTs transfer fucose to the terminal Gal*β* unit of precursor chains type 1 (Gal*β*1,3GlcNAc) or type 2 (Gal*β*1,4GlcNAc) to form H antigens. At least two distinct α1,2-FucTs, FUT1 and FUT2, are restricted to specific tissues. FUT1 is active mainly in erythrocyte membranes, whereas FUT2 is detected mainly in epithelial cells and in body fluids such as saliva (*14*). A third gene in humans called *SEC1* appears to be a pseudogene with inactivating frame-shift mutations (*15*). The counterparts of human α1,2-FucTs were also found in

* Corresponding author. Tel: 614-292-9884. Fax: 614-292-6773. E-mail: wang.892@osu.edu.

‡ Wayne State University.

§ Present address: Department of Microbiology, University of Alabama at Birmingham, Birmingham, AL 35294.

‖ The Ohio State University.

⊥ Exchange student from College of Life Science, Shandong University, Jinan, Shandong 250100, P. R. China.

[1] Abbreviations: FucT, fucosyltransferase; GDP, guanosine 5′-diphosphate; Fuc, fucose; Fru, fructose; Gal, galactose; Glc, glucose; Man, mannose; GalNAc, *N*-acetylgalactosamine; GlcNAc, *N*-acetylglucosamine; LacNAc, *N*-acetyllactosamine; GST, glutathione S-transferase; IPTG: isopropyl-1-thio-*β*-D-galactospyranoside; DTT, dithiothreitol; AP, alkaline phosphatase; HRP, horseradish peroxidase; TLC, thin layer chromatography; MS, mass spectrometry; NMR, nuclear magnetic resonance.

10.1021/bi701345v CCC: $40.75
Published on Web 12/14/2007

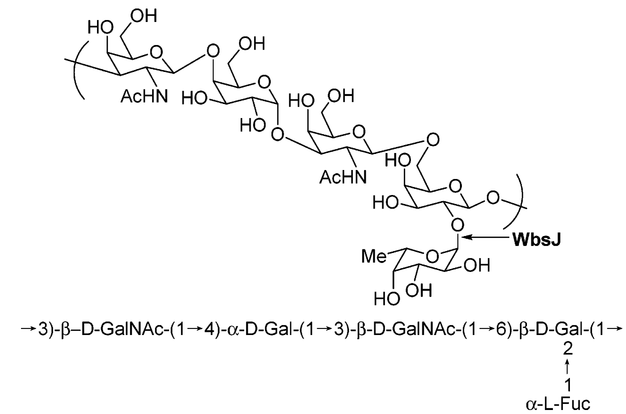

FIGURE 1: Structure of *E. coli* O128:B12 O-antigen repeating unit. WbsJ: α1,2-fucosyltransferase.

specific tissues of mice and rats (*11*, *16*). In prokaryotes, *Hp fucT2* from the pathogenic bacterium *Helicobacter pylori* has been cloned and found to encode an α1,2-FucT involved in the synthesis of oncofetal antigen Lewis Y (*17*). This is the first and only bacterial α1,2-FucT biochemically characterized thus far. In contrast to mammalian α1,2-FucTs, *Hp fucT2* prefers Lewis X [Galβ1,4(Fucα1,3)GlcNAcβ-R] rather than LacNAc (Galβ1,4GlcNAcβ-R) as the acceptor (*17*).

The enterpathogenic strain *Escherichia coli* (EPEC) O128 is associated with infantile diarrhea, one of the major causes of illness and death among children in developing countries (*18*). The O-antigens (O-specific polysaccharide) are the exposed part of the lipopolysaccharides (LPS), the major outer-membrane component of Gram-negative bacteria (*19*). Variations of O-antigens contribute to the wide variety of antigenic types of different bacterial species. O-antigens are furthermore recognized as important virulence factors (*20*) and have the potential to influence host−pathogen interactions in many different ways. Molecular mimicry, for example, can protect the pathogens from host antigen-specific immune defenses (*19*, *21*).

The primary structure of the O-antigen repeating unit of *E. coli* O128 has been determined as a −[3GalNAcβ1,4Galα1,3GalNAcβ1,6(Fucα1,2)Galβ1]− pentasaccharide (Figure 1) (*18*), in which Fucα1,2Galβ− was reported to be the immunodominant part (*22*). Previously, we reported the sequence of the *E. coli* O128:B12 O-antigen biosynthesis gene cluster and biochemical identification of an α1,2-FucT encoded by the *wbsJ* gene (GenBank No. AY217096) of this cluster (*23*). Sequence analysis indicated low sequence similarity among various α1,2-FucT homologues; however, they all share three conserved motifs (motif I, II and III) with α1,6-FucTs (*24*, *25*). Intensive research on α1,3-FucTs from bacteria (*26*−*28*) and α1,6-FucTs from porcine (*29*), human (*30*), and bacterial *Rhizobium* species (*5*) have been carried out to understand the mechanism of FucTs. Very recently, the crystal structures of *H. pylori* α1,3-FucT (*28*) and mammalian α1,6-FucT (*31*) were solved. However, much less effort has been made to investigate the properties of α1,2-FucT, especially bacterial α1,2-FucT. Herein we report the detailed biochemical characterization of a recombinant α1,2-FucT (WbsJ) from *E. coli* O128:B12. This novel bacterial α1,2-FucT shows broad acceptor specificity with Galβ1,4Fru (lactulose), Galβ1,4Glc (lactose), Galβ1,3GalNAc and Galβ1,4Man all being good acceptors. The broad acceptor specificity also reveals its potential application in the synthesis of important fucosylated glycoconjugates. We additionally investigated the requirement of divalent metal ions on the enzyme activity. Furthermore, secondary structure predictions indicated that WbsJ belongs to the GT-B-like superfamily. Finally, the function of the highly conserved HxRRxD motif was investigated by mutagenesis and kinetic studies. This is the first report of the enzymatic characterization and kinetic studies of a bacterial α1,2-FucT. In addition, the application of WbsJ in the synthesis of fucosylated oligosaccharides was explored.

MATERIALS AND METHODS

Cloning and Construction of wbsJ from E. coli O128:B12. The *wbsJ* gene was amplified by polymerase chain reaction (PCR) from chromosomal DNA of *E. coli* O128:B12 with the forward primer 5′-CGCGGATCC*ATG*GAAGTTAAAATTATTGGGGGGCT-3′ (*Bam*HI restriction site underlined, start codon in italic type) and the reverse primer 5′-CGGAATTCTCGAG*TCA*TAATTTTACCCACGATTCG-3′ (*Xho*I restriction sites underlined, stop codon in italic type). The PCR fragment was digested with *Bam*HI and *Xho*I and inserted into the *Bam*HI/*Xho*I sites of plasmid pGEX-4T-1 such that the resultant expression plasmid pGEX-wbsJ had *wbsJ* fused to the gene encoding glutathione S-transferase (GST) in the same open reading frame under the control of the P_{tac} promoter. The constructs were subsequently transformed into *E. coli* DH5α cells. Selected clones were characterized by restriction mapping and DNA sequencing. The correct constructs were subsequently transformed into *E. coli* BL21 (DE3) for protein expression.

Site-Directed Mutagenesis. Site-directed mutagenesis was performed by two methods using plasmid pGEX-wbsJ as the template. Mutants H152A, R154A and D157N were generated by two-step PCR. The rest of the mutants were generated using the QuikChange site-directed mutagenesis kit (Stratagene, La Jolla, CA) following the manufacturer's instructions. All primers used for mutagenesis are listed in Table 1. The constructed mutations were confirmed by DNA sequencing.

Overexpression and Enzyme Purification. E. coli BL21 (DE3) strains harboring the recombinant plasmid, including the wild-type and mutants, were grown in 1 L of LB medium with shaking at 220 rpm at 37 °C. When OD_{600} reached 0.8, isopropyl-1-thio-β-D-galactospyranoside (IPTG) was added to a final concentration of 1 mM for induction, after which expression was allowed to proceed for 6 h at 30 °C. Cells were harvested by centrifugation at 4 °C and stored at −80 °C until needed.

The cell pellet was suspended in GST binding buffer (140 mM NaCl, 2.7 mM KCl, 10 mM Na_2HPO_4, 1.8 mM KH_2PO_4, pH 7.3) and disrupted by sonication on ice. The lysate was cleared by centrifugation (10000*g*, 30 min) and the supernatant was loaded onto a 5 mL GSTrap FF column (GE Healthcare Life Sciences, Piscataway, NJ), followed by washing with the same buffer. The protein was subsequently eluted with GST elution buffer (50 mM Tris-HCl, 10 mM reduced glutathione, pH 8.0). The eluted protein was nearly homogeneous by 12% SDS−PAGE analysis. For wild type GST-WbsJ, further purification was carried out by gel filtration chromatography on a HiLoad 16/60 Superdex 200

Table 1: WbsJ Mutants and Sequences of Primers Used for Site-Directed Mutagenesis[a]

mutants	primer sequence
H152A	5′-TGATACTTGTTCATTAGCAATTAGAAGAGGTGATTA-3′
	5′-TAATCACCTCTTCTAATTGCTAATGAACAAGTATCA-3′
H152R	5′-ATGATACTTGTTCATTAAGAATTAGAAGAGGTGATTATG-3′
	5′-CATAATCACCTCTTCTAATTCTTAATGAACAAGTATCAT-3′
R154A	5′-CTTGTTCATTACATATTGCAAGAGGTGATTATGTTTCC-3′
	5′-GGAAACATAATCACCTCTTGCAATATGTAATGAACAAG-3′
R154K	5′-TGTTCATTACATATTAAAAGAGGTGATTATGTTT-3′
	5′-AAACATAATCACCTCTTTTAATATGTAATGAACA-3′
R155A	5′-GTTCATTACATATTAGAGCAGGTGATTATGTTTCCAGT-3′
	5′-ACTGGAAACATAATCACCTGCTCTAATATGTAATGAAC-3′
R155K	5′-TCATTACATATTAGAAAAGGTGATTATGTTTCCA-3′
	5′-TGGAAACATAATCACCTTTTCTAATATGTAATGA-3′
D157A	5′-TACATATTAGAAGAGGTGCATATGTTTCCAGTAAAAT-3′
	5′-ATTTTACTGGAAACATATGCACCTCTTCTAATATGTA-3′
D157E	5′-ACATATTAGAAGAGGTGAATATGTTTCCAGTAAAATAG-3′
	5′-CTATTTTACTGGAAACATATTCACCTCTTCTAATATGT-3′
D157N	5′-TACATATTAGAAGAGGTAATTATGTTTCCAGTAAAA-3′
	5′-TTTTACTGGAAACATAATTACCTCTTCTAATATGTA-3′

[a] The sequences of mutant residues are underlined.

prep grade column (GE Healthcare Life Sciences) with an AKTA FPLC system (GE Healthcare Life Sciences). Tris-HCl buffer (50 mM, pH 7.4) containing 2 mM DTT and 100 mM NaCl was used for equilibration and elution.

Fucosyltransferase Activity Assay. Enzyme activity was determined at 37 °C for 2 h in a final volume of 50 μL containing 40 mM Tris-HCl (pH 7.4), 1 mM DTT, 0.3 mM GDP-β-L-fucose, GDP-L-[U-^{14}C]fucose (7000 cpm), 20 mM acceptor and 10 μg of enzyme. The acceptor was omitted in the control reaction. The reaction was stopped by adding 150 μL of ice cold water. Dowex 1× 8-400 anion exchange resin (Sigma-Aldrich, St. Louis, MO) was then added as a water suspension (0.8 mL, v/v = 1/1). After centrifugation, the supernatant (0.5 mL) was collected in a 20-mL plastic vial to which 10 mL of Scintiverse BD (Fisher Scientific, Pittsburgh, PA) was added. The vial was vortexed thoroughly before the radioactivity of the mixture was counted in a Beckmann LS-3801 liquid scintillation counter (Beckman Instruments, Fullerton, CA). Protein concentration was quantified by the Bradford assay using Bio-Rad Protein Assay reagents (Bio-Rad, Hercules, CA) with standard solutions of BSA.

The activities of α1,2-FucT at different pH conditions were determined with 10 μg of recombinant GST-WbsJ in 50 μL of a solution under differing pH conditions (pH 4.2−9.5), 0.3 mM GDP-fucose and 15 mM lactose for 1 h.

Kinetic Analysis of Recombinant GST-WbsJ. Kinetic analysis of GST-WbsJ was performed at 37 °C for 1 h in 40 mM Tris-HCl buffer (pH 7.4) containing 1 mM DTT and 10 μg of enzyme. To determine apparent K_m values for acceptors, the concentration of acceptors was varied and the reaction assays were performed using 0.3 mM GDP-fucose and 3 μM GDP-L-[U-^{14}C]fucose, in which the product was measured via scintillation counting. To determine the apparent K_m value for GDP-fucose, 3 μM GDP-L-[U-^{14}C]fucose was supplemented with different amounts of unlabeled GDP-fucose to achieve various GDP-fucose concentrations (0.02, 0.04, 0.08, 0.16, 0.32 and 0.40 mM) with a fixed acceptor concentration of 20 mM. The parameters $^{app}K_m$ and $^{app}V_{max}$ were obtained by plotting initial velocity versus substrate concentration and curve-fitting to the Michaelis−Menten equation with nonlinear regression using the program KaleidaGraph 3.0. The inhibitor binding constant K_i of GDP to α1,2-FucT was determined by an activity assay using various concentration of the acceptor (0.8, 1.6, 3.2, 4 and 8 mM) and a fixed concentration of the donor (0.3 mM) with and without the addition of GDP at different concentrations (0, 0.6, 1.0 and 2.0 mM).

Western Blot Analysis. After resolving by 12% SDS−PAGE, proteins were transferred onto a Hybond-C Extra Nitrocellulose Membrane (GE Healthcare Life Sciences) followed by blocking with 5% nonfat dry milk in TBS-T buffer (20 mM Tris-HCl, 150 mM NaCl, 0.05% Tween-20, pH 7.4). All the incubations were conducted at room temperature for 1 h followed by washing three times for 10 min each with TBS-T buffer. The GST fusion protein was detected by incubation with mouse anti-GST monoclonal IgG (EMD Chemicals, San Diego, CA) at 1:500 dilution. Either alkaline phosphatase (AP)-conjugated (GE Healthcare Life Sciences) or horseradish peroxidase (HRP)-conjugated goat anti-mouse IgG (Santa Cruz Biotechnology, Santa Cruz, CA) was then used as the secondary antibody at a dilution of 1:2000. The blot was developed directly either via treatment with BCIP (5-bromo-4-chloro-3-indoyl phosphate) and NBT (nitro-blue tetrazoline) for AP-conjugated secondary antibody, or via treatment with ECL Western Blotting Detection Reagent (GE Healthcare Life Sciences) followed by exposure to CL-Xposure Clear Blue X-ray film (Pierce Biotechnology, Rockford, IL) for HRP-conjugated secondary antibody.

GDP-bead Binding Assay. A 30 μL aliquot of Glycosyltransferase Affinity Gel-GDP (10 μmol GDP/mL gel slurry, EMD Chemicals) was washed three times with binding buffer (50 mM Tris-HCl, 5% glycerol, 100 mM NaCl, 5.0 mM $MgCl_2$, 1 mM DTT, pH 7.0). The beads were incubated on a roller at 4 °C for 1 h with 40 μL of purified recombinant wild-type WbsJ and its variant mutants in the binding buffer. To evaluate the potential factors influencing GDP binding, incubations were performed in the presence of $MnCl_2$ (10 mM), GDP (25 mM) or L-fucose (25 mM) respectively. Finally, the beads were harvested by centrifugation for 1 min at 1000*g*, after which they were washed three times with binding buffer and boiled with SDS−PAGE loading buffer for 5 min. The bound enzymes were analyzed by SDS−PAGE followed by Western blot as described above.

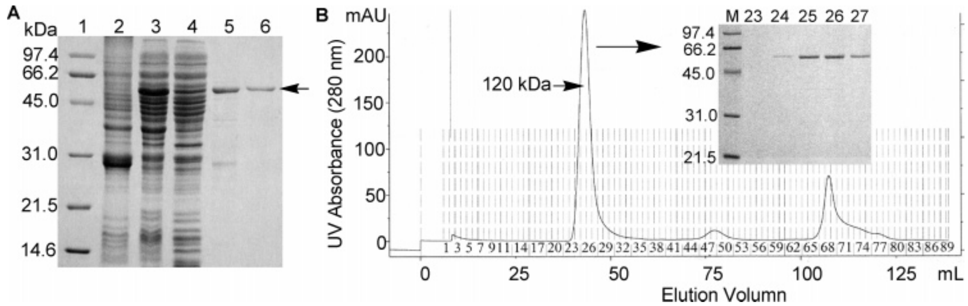

FIGURE 2: Expression and purification of GST-WbsJ fusion protein. (A) SDS−PAGE analysis of GST-WbsJ expression and purification. Lane 1: molecular weight marker. Lane 2: cell extract of *E. coli* BL21 (DE3) with pGEX-4T-1. Lane 3: cell extract of *E. coli* BL21 (DE3) expressing GST-WbsJ. Lane 4: cell lysate of GST-WbsJ. Lane 5: eluted protein from GST affinity chromatography. Lane 6: purified GST-WbsJ through size exclusion chromatography. The bands indicated with an arrow were GST-WbsJ. (B) Elution profile of size exclusion chromatography and SDS−PAGE of elution fractions (fraction #23−27) of first peak. The molecular weight of native GST-WbsJ (the first peak) was determined to be 120 kDa by comparison with the elution volumes of standard proteins under the same conditions (flow rate 0.5 mL/min). The first peak is purified native GST-WbsJ, corresponding to the molecular weight of 60 kDa in the denaturing 12% SDS−PAGE (M: molecular marker).

Enzymatic Synthesis of Fucosylated Saccharides. Preparative reactions in milligram scale were conducted with Galβ-*O*-Me and Galβ1,4Glcβ-N_3 as acceptors, respectively. The reactions were optimized so that the maximum of substrate was converted to the product. Briefly, the reaction was conducted at 30 °C in a final volume of 2.0 mL containing 40 mM Tris−HCl (pH 7.4), 1 mM DTT, 10 mM GDP-fucose, and 15 mM acceptor. The reaction was initiated by addition of 2 mg α1,2-FucT. The progress of the reaction was monitored by thin-layer chromatography [*i*-PrOH/H_2O/NH_4OH = 7:3:2 (v/v/v)] conducted on Baker Si250F silica gel TLC plates with a fluorescent indicator. Products were visualized by staining with anisaldehyde/MeOH/H_2SO_4 = 1:15:2 (v/v/v). After complete conversion of donor substrate to product, proteins were removed by brief boiling, followed by centrifugation (12000*g*, 20 min). Finally, oligosaccharide products were separated and purified by Bio-Gel P-2 gel filtration (Bio-Rad) with water as the mobile phase. The desired fractions were pooled, lyophilized, and stored at −20 °C.

Mass Spectrometry and NMR. Electrospray ionization mass spectrometry (ESI-MS) assays were conducted using a Micromass Quattro LC mass spectrometer. ^{1}H and ^{13}C NMR spectra were recorded on a 500 MHz Varian VXR500 NMR spectrometer. Product structures were identified by one-dimensional (selective COSY, relay COSY, and NOE) and two-dimensional (COSY, HMQC, NOESY, and HMBC) ^{1}H/^{13}C NMR. The oligosaccharide products were repeatedly dissolved in D_2O and lyophilized before the NMR spectra were recorded at 303 K in a 5 mm tube.

RESULTS

Expression and Purification of Recombinant WbsJ. Due to earlier failures in purifying recombinant WbsJ with a His_6 tag using either plasmid pET-15b or pET-23a, pGEX-4T-1 was chosen to express *wbsJ* with a GST tag in order to improve enzyme solubility and stability. After successful insertion of the *wbsJ* gene into the pGEX-4T-1 vector, the recombinant *wbsJ* gene was overexpressed in *E. coli* BL21 (DE3) upon the induction of 1 mM IPTG at 30 °C. The fusion protein GST-WbsJ was produced with a GST tag at the N-terminus and was purified to >95% in one-step by GST affinity chromatography. Further elimination of impurities by size exclusion chromatography produced pure protein as shown by SDS−PAGE (Figure 2A). The fusion protein has a high theoretical isoelectric point (pI = 8.6) and an apparent molecular weight of 60 kDa as estimated by SDS−PAGE, similar to the theoretical value (59 806 Da) calculated from its predicted amino acid sequence.

The molecular weight of native fusion GST-WbsJ is approximately 120 kDa, as shown in gel filtration profile, indicating that the fusion protein is a homodimer (Figure 2B). This observation must have arisen due to the fact that active GST exists as a homodimer in nature. Attempts to cleave the GST tag from the fusion protein with thrombin were unsuccessful. The cleavage efficiency is low (about 20−30%), and about 20% of the cleavage product results from nonspecific cleavage. This indicates that the N-terminus of WbsJ may form a conformation which is not readily accessed by thrombin. The two forms of the WbsJ enzyme (free and fusion forms) were compared using a radioactive assay with the same acceptors. The results showed that the relative activities had no significant difference (data not shown). However, the free WbsJ, especially the mutant, is less stable and the yield of thrombin cleavage is low. Thus we chose the fusion form to conduct biochemical studies.

Detection of α1,2-FucT Activity and Substrate Specificity of GST-WbsJ. The α1,2-FucT activity and substrate specificity of GST-WbsJ were studied. Based on the O-antigen structure, a panel of oligosaccharides and their derivatives were selected. The results showed broad acceptor specificity of WbsJ (Table 2). Galβ1,3GalNAc (blood group T antigen), Galβ1,4Man and Galβ1,4Glc (lactose) are better acceptors than Galβ-*O*-Me. Galβ1,4Fru (lactulose), a natural sugar, was shown to be the best acceptor with a reaction rate nearly four times faster than that of lactose. Replacement of the reducing terminal Glc with GlcNAc made it a very poor substrate, however. Compounds with a terminal α-Gal did not serve as acceptors. Furthermore, it appears that the C2-OH of Glc (in lactose) is important for enzyme recognition because the enzyme activity of LacNAc is only 12.4% compared with that of lactose. It is also interesting to note that the difference between Galβ1,4Gal and Galβ1,4Man is at the C2-OH of the reducing-end sugar moiety. The C2-OH of Gal is in the equatorial conformation whereas the C2-OH of Man is in the axial conformation. This observation may help to explain the fact that the enzymatic activities

Table 2: Acceptor−Substrate Specificity of Purified GST-WbsJ[a]

acceptor (10 mM)	rel act. (%)	acceptor (10 mM)	rel act. (%)
Gal*β*1,4Glc (lactose)	**100 ± 1.4**	Gal	35.7 ± 1.1
Gal*β*1,4Glc*β*-N_3 ($LacN_3$)[b]	137 ± 3.7	Gal*β*-*O*-Me	68.8 ± 4.0
Gal*β*1,4Glc*β*-*O*-ph	84.7 ± 4.3	Gal*β*1,4GlcNAc	12.4 ± 0.2
Gal*β*1,4Glc*β*-S-ph	207 ± 9.7	**Gal*β*1,4Fru (lactulose)**	**380 ± 14.9**
Gal*β*1,4Glc*β*−1-NAc	199 ± 11.2	Gal*β*1,4Gal	ND
Galα1,4Gal	ND	**Gal*β*1,4Man**	**162 ± 4.7**
Galα1,4Gal*β*1,4Glc	ND	**Gal*β*1,3GalNAcα-*O*-Bn (T antigen)**	**202 ± 6.7**
Galα1,3Gal*β*1,4Glc	ND	**Gal*β*1,3GalNAcα-*O*-Me (T antigen)**	**215 ± 5.9**
Galα-PNP	ND	GalNAc*β*1,3Galα1,4Gal*β*1,4Glc	ND
Gal*β*-PNP	30.4 ± 0.7		

[a] The α1,2-fucosyltransferase activities of GST-WbsJ with different acceptors were determined at 37 °C for 2 h containing 20 mM Tris-HCl, pH 7.0, 1 mM ATP, 0.3 mM GDP-*β*-L-fucose, GDP-L-[U-[14]C]fucose (7000 cpm), 20 mM acceptor and 10 μgof enzyme. The acceptors showing high enzyme activities are highlighted in bold. The results are from two parallel experiments. [b] Abbreviations: rel act., relative activity; Gal, galactose; Glc, glucose; Fru, fructose; Man, mannose; GalNAc, *N*-acetylgalactosamine; GlcNAc, *N*-acetylglucosamine; Bn, benzyl; Me, methyl; N_3: azide group; NAc, *N*-acetyl amine; ph, phenyl; PNP, *p*-nitrophenol; ND, not detectable.

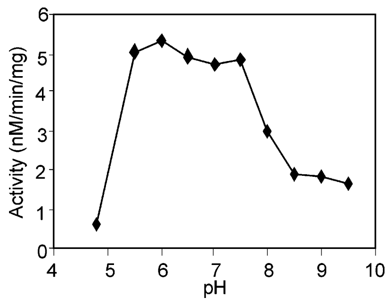

FIGURE 3: Effect of pH on α1,2-fucosyltranferase activity of GST-WbsJ.

are remarkably different (Gal*β*1,4Gal, 0%; Gal*β*1,4Man, 162%).

Optimal pH Conditions for α1,2-FucT Activity of GST-WbsJ. The activity of α1,2-FucT was determined under different pH conditions at 37 °C with lactose as the acceptor. The pH profile showed a sort of "bell shape" curve. The enzyme was active within a wide range of pH values (5.5−8.5) (Figure 3), with the highest activity occurring within the pH range of 6−7.4. The optimum observed may be due to a pH effect on ionization of the catalytic residue, on binding affinity, on the stability of the enzyme, or a combination of these effects (*32*).

Metal Ion Effect on α1,2-FucT Activity. Glycosyltransferases of the GT-A superfamily share a conserved DXD or EXD motif and exhibit the requirement for divalent metal cations for catalysis (*33*). Glycosyltransferases of the GT-B superfamily do not have this motif, and most of them do not need metal ions for activity (*34*, *35*). The effects of EDTA and various divalent metal cations on WbsJ activity were investigated. The results indicated that the α1,2-FucT activity of WbsJ was independent of divalent metal ions. The enzyme activity was at approximately the same level with 10 mM EDTA and Mg^{2+} (Figure 4). In accordance with the results, sequence analysis of WbsJ indicated the absence of a DXD motif. Milder inhibition was observed with the addition of 10 mM Mn^{2+} and Ca^{2+}. Enzyme activity was severely inhibited by Cu^{2+}, Zn^{2+}, and Ni^{2+} ions. Although Mn^{2+} and Mg^{2+} ions are not essential, further investigation found that they stimulate enzyme activity slightly (4−11%) at lower concentrations (<5 mM for Mn^{2+}, <10 mM for Mg^{2+}), but show inhibition at higher concentrations (>15 mM, data not shown). The same observation was made with

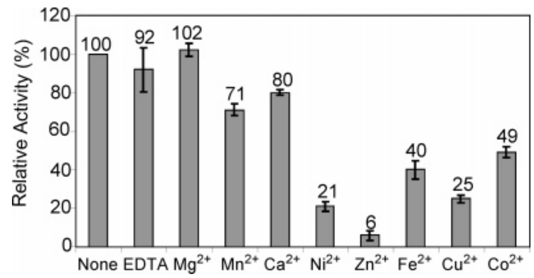

FIGURE 4: Effect of divalent metal ion on α1,2-fucosyltranferase activity of GST-WbsJ. The concentrations of EDTA and the divalent metal cations were 10 mM. The reaction without addition of metal ion and EDTA is labeled as none.

α1,2-FucT from porcine (*36*), but not in human α1,6-FucTs FUT8 (*37*).

Inhibition of α1,2-FucT Activity by GDP. Byproduct inhibition is a factor that limits the yield of enzymatic synthesis of oligosaccharides (*38*). The inhibition of fucosyltransferases (α1,2-, α1,3- and α1,6-FucT) by GDP has been reported (*39*−*41*). Therefore, the effects of sugar nucleotides on the α1,2-fucosyltransferase activity of GST-WbsJ were analyzed using lactulose as the acceptor, in the presence or absence of the following substrates: ATP, ADP, AMP, GTP, GDP, GMP and L-α-fucose at concentrations of 1 mM. Enzyme activity was severely inhibited by GDP at 1 mM. ATP, ADP, AMP, and L-α-fucose did not inhibit enzyme activity at this concentration. Kinetic studies revealed that WbsJ is competitively inhibited by GDP with an apparent K_i value of 1.41 mM (Figure 5).

Effect of Mutations of Common Motif on α1,2-FucT Activity. Sequence alignment of α-1,2 FucTs of various species reveals a highly conserved motif, HxRRxD, which is rich in basic residues (Figure 6). This motif is found in both the α1,2-FucT family and the α1,6-FucT family. The presence of this highly conserved motif suggests that it may play important roles in the binding of donor GDP-fucose or enzyme catalysis. To investigate the functions of this motif, nine mutants were constructed by site-directed mutagenesis at residues H^{152} (A or R), R^{154} (A or K), R^{155} (A or K) and D^{157} (A, E or N). Most of the mutants were expressed at a similar level to the wild-type enzyme except for mutants R154K, R155A, and R155K, whose expression levels were approximately two times higher than that of the wild-type enzyme (Figure 7A). All of the mutants were purified via a

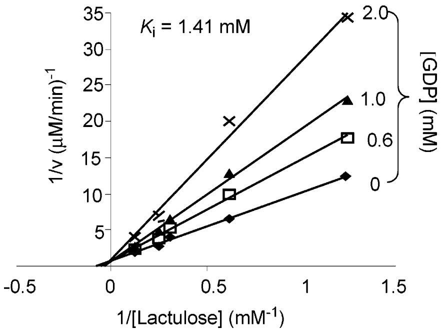

FIGURE 5: GDP inhibition on the α1,2-fucosyltranferase activity of GST-WbsJ with lactulose as the acceptor. The K_i value of GDP for GST-WbsJ was obtained by varying the concentration of acceptor (lactulose) at different concentrations of GDP (0, 0.6, 1.0 and 2.0 mM) with a fixed donor (GDP-fucose) concentration (0.30 mM).

GST affinity column (Figure 7B). As is shown from the Coomassie blue stained SDS−PAGE (Figure 7B), the protein purified through GST affinity chromatography contains two major impurities with molecular weight of 29 kDa and 39 kDa, respectively. The identities of these two major impurities were analyzed by mass spectrometry using trypsin in-gel digestion. The band at 29 kDa is the truncated GST protein moiety and the one at 39 kDa is OmpF, the out membrane protein F of *E. coli* (data not shown). While the impurity should not affect the enzyme activity, it would affect the measurement of enzyme concentration. Therefore, the protein concentrations of wild type and mutant GST-WbsJ were normalized by quantifying protein bands on Coomassie brilliant blue stained SDS−PAGE using Image Quant software, with homogenously purified wild type GST-WbsJ protein as a standard.

Specific enzyme activities of the mutants were measured and compared with the wild type using lactulose as the acceptor (Figure 7C). Substitution of H^{152} by either Ala (A) or Arg (R) decreased the enzyme activity to 19.2% or 11.5% of the wild type. Mutation R154A resulted in marginal activity (3% of the wild type), compared with the complete loss of activity seen in the α1,6-FucTs with equivalent mutations. Moreover, conservative replacement of R^{154} by the positively charged residue Lys (K) was able to restore activity to 12.0%. This result indicates that both the positive charge and the size of side chain of R^{154} are critical for α1,2-FucT activity. Adjacent to R^{154}, the mutation of R155A resulted in significant reduction of activity (15.4%), whereas the conservative mutation of R155K restored the activity to 31.1%, suggesting that R^{155} may play a less important role than R^{154}. In motif HxRRxD, the last conserved residue D^{157} was changed to Ala (A), Glu (E) or Asn (N). All three mutants D157A, D157E and D157N exhibited very low, but still detectable, levels of activity (4.1%, 6.8% and 5.3%, respectively). Replacement with a similar acidic residue (D175E) caused no remarkable difference in activity compared with D157A. Overall, the above results indicate that, within this conserved motif, R154 and D157 play more important roles than other residues.

Kinetic Analysis of Mutants. The kinetic parameters of seven mutants (H152A, H152R, R154K, R155A and R155K), which possessed higher enzyme activities were determined with GDP-fucose as the donor and lactulose as the acceptor. Mutant H152A gave an apparent K_m value for donor GDP-fucose which was twice as large as of the value for H152R (Table 4). This result indicated the need for a positive residue at this position. The change of H^{152} to R also resulted in a significant increase of the K_m value for the acceptor, probably because the bulky side chain of Arg interferes with binding of the acceptor, leading to weaker binding affinity. Mutants R155A and R155K showed similar K_m values for the acceptor (76.0 mM and 64.8 mM, respectively). However, mutant R155A, which eliminates the positive charge, yielded a K_m value for the donor substrate three times greater than that of mutant R155K. These results suggest that preservation of the positive charge at residue R^{155} is more important than the length of the side chain for the binding of GDP-fucose as well as enzyme function. This data is consistent with the results of the specific enzyme activities of the mutants.

Effects of Mutations on Binding of α1,2-FucT to GDP-beads. To further investigate the roles of conserved residues of motif I in binding to the nucleotide moiety, GDP-bead binding analysis was performed with both wild-type and mutant FucTs. The wild-type enzyme bound to GDP-beads with a slightly higher affinity in the presence of Mn^{2+}. The binding was inhibited by 25 mM GDP but not L-fucose at the same concentration (Figure 8A). In agreement with the inhibition experiments, it implies that α1,2-FucT predominantly recognizes the GDP moiety rather than the sugar moiety.

All nine mutants showed the ability to bind to GDP-beads, although some of them have dramatically impaired enzyme activities (R154A, D157A, D157E and D157N) (Figure 8B). Using Image Quant software we were able to quantify individual protein bands and obtain the relative GDP binding ability by comparison of the amount of mutant protein binding to GDP-beads with that of the wild type. H152R, R154A, and D157N showed remarkablely decreased GDP binding abilities with relative activities of 53%, 42%, and 43%, respectively (Figure 8B). In contrast, H152A, R154K, D157A and D157E displayed moderate decreased binding activities (66−75%). It seems that mutations at residue of R^{155} (R155A and R155K) do not affect enzyme binding to the GDP moiety.

Synthesis of Fucosylated Oligosaccharides. Purified GST-WbsJ was employed for milligram scale synthesis with GDP-fucose as the donor, along with Gal*β*-*O*-Me and Gal*β*1,-4Glc*β*-N_3 as acceptors, respectively. A total of 4.4 mg of Fucα1,2Gal*β*-*O*-Me (yield 71%) and 5.2 mg of Fucα1,2 Gal*β*1,4Glc*β*-N_3 (yield 78%) were obtained.

The purified products were subjected to ESI-MS analysis. The ESI-MS of Fucα1,2Gal*β*-*O*-Me showed two prominent peaks of $(M + Na)^+$ at m/z 363.1 and $(M + K)^+$ at m/z 379.1, which were interpreted based on the predicted molecular weight of 340.14 (see the Supporting Information, Figure S1). For trisaccharide Fucα1,2Gal*β*1,4Glc*β*-N_3, the prominent peak at m/z 536.26 is interpreted as the $(M + Na)^+$ of the parent compound, given the predicted molecular weight of 513.18 (Figure S2).

NMR analysis of these two fucosylated oligosaccharides was also performed to confirm the product (for spectra, see the Supporting Information).

Fucα1,2Galβ-O-Me: ^{1}H NMR (500 MHz, D_2O) δ 4.95 (d, J = 4.0 Hz, 1H), 4.24 (d, J = 7.5 Hz, 1H), 4.09 (dd, J_1 = 6.5 Hz, J_2 = 13.5 Hz, 1H), 3.74 (d, J = 3.0 Hz, 1H), 3.70 (dd, J_1 = 4.0 Hz, J_2 = 11.0 Hz, 1H), 3.67 (dd, J_1 = 3.5 Hz,

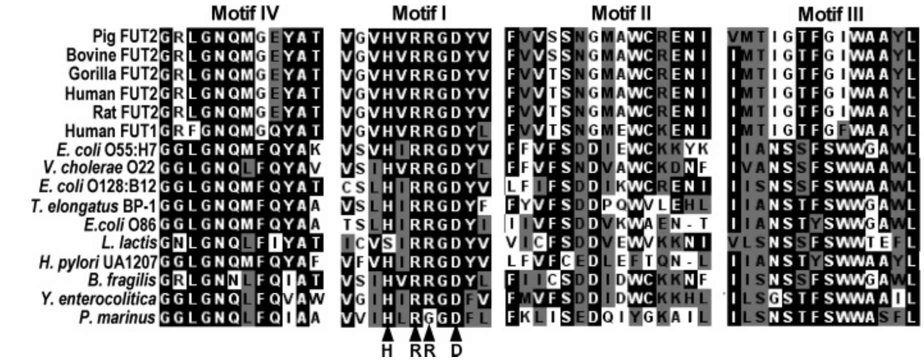

FIGURE 6: Conserved motifs of α1,2-FucTs from bacteria and mammals. The white letters with black background represent identical amino acids, while black letters with gray background represent similar amino acids conserved in all aligned sequences. The conserved motifs I, II, III and IV were in the order from N-terminus to C-terminus. The conserved residues of motif I ($H^{152}xR^{154}R^{155}xD^{157}$) which were replaced by mutagenesis were labeled with triangles. *E. coli*, *Escherichia coli*; *V. cholerae*, *Vibrio cholerae*; *T. elongatus*, *Thermosynechococcus elongatus*; *L. lactis*, *Lactococcus lactis*; *H. pylori*, *Helicobacter pylori*; *B. fragilis*, *Bacteroides fragilis*; *Y. enterocolitica*, *Yersinia enterocolitica*; *P. marinus*, *Prochlorococcus marinus*. All GenPept accession loci of these protein sequences can be found at http://www.cazy.org/fam/GT11.html.

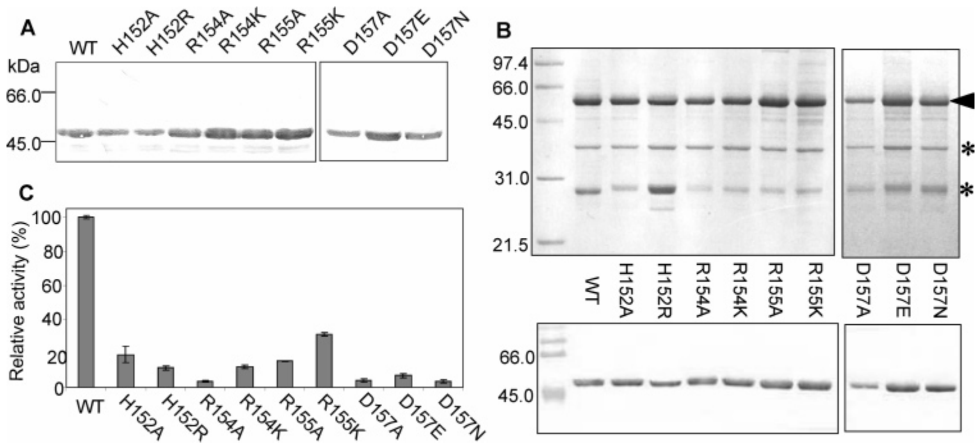

FIGURE 7: Expression, purification and activity of GST-WbsJ mutants compared with the wild type. (A) Western blot analysis of protein expression of mutant and wild type GST-WbsJ in *E. coli* BL21 (DE3). (B) SDS−PAGE (upper panel) and Western blot (lower panel) analysis of wild type and mutant GST-WbsJ purified by GST affinity chromatography. SDS−PAGE was performed on 12% gel. The arrow represents the GST-WbsJ protein. The stars represent the impure proteins. (C) The relative activities of GST-WbsJ mutants compared with the wild type. WT: wild type.

Table 3: Kinetic Parameters of Recombinant GST-WbsJ[a]

substrate	${}^{app}K_m$ (mM)	${}^{app}V_{max}$ (μM/min)	k_{cat} (min^{-1})	$k_{cat}/{}^{app}K_m$ (M^{-1}·min^{-1})
Galβ-*O*-Me	59.62 ± 2.36	0.083 ± 0.014	0.0173	0.29
lactose	7.81 ± 0.96	0.239 ± 0.057	0.0497	6.36
lactulose	13.26 ± 0.74	1.311 ± 0.125	0.151	13.39
GDP-fucose	0.106 ± 0.032	0.702 ± 0.08	0.131	1235

[a] Kinetic analysis of GST-WbsJ was performed at 37 °C for 1 h in 40 mM Tris-HCl buffer (pH 7.4) containing 1 mM DTT and 10 μg of enzyme. To determine apparent K_m values, either the concentration of acceptor was varied with a fixed concentration of donor GDP-fucose at 0.3 mM or the concentration of GDP-fucose was changed with a fixed concentration of acceptor at 20 mM.

Table 4: Kinetic Parameters of GST-WbsJ Mutants Compared with the Wild Type[a]

	lactulose		GDP-fucose	
enzyme	${}^{app}K_m$ (mM)	${}^{app}V_{max}$ (μM/min/mg)	${}^{app}K_m$ (mM)	${}^{app}V_{max}$ (μM/min/mg)
wild type	14.4 ± 1.1	9.1 ± 1.4	0.122 ± 0.005	12.8 ± 0.2
H152A	55.3 ± 9.3	2.8 ± 0.3	0.865 ± 0.150	5.6 ± 0.7
H152R	96.7 ± 24.3	5.7 ± 0.8	0.462 ± 0.140	3.5 ± 19.1
R154K	108 ± 27.6	5.5 ± 0.9	0.575 ± 0.070	8.4 ± 0.7
R155A	76.0 ± 7.3	5.5 ± 0.3	1.997 ± 0.640	12.1 ± 3.4
R155K	64.8 ± 6.5	1.9 ± 0.1	0.628 ± 0.271	5.2 ± 1.4

[a] Kinetic analyses of GST-WbsJ mutants were performed using the same method as described in Table 3.

J_2 = 10.0 Hz, 1H), 3.64−3.59 (m, 4 H), 3.51 (dd, J_1 = 4.0 Hz, J_2 = 7.5 Hz, 1H), 3.41 (s, 3H), 3.34 (dd, J_1 = 8.5 Hz, J_2 = 9.5 Hz, 1H), 1.04 (d, J = 6.5 Hz, 3H); ^{13}C NMR (125 MHz, D_2O) δ 102.9, 100.2, 78.3, 75.1, 73.4, 72.1, 69.7, 68.6, 67.0, 61.1 57.3, 15.3.

*Fuc*α*1,2Gal*β*1,4Glc*β*-N*$_3$: ^{1}H NMR (500 MHz, D_2O) δ 5.33 (d, J = 3.4 Hz, 1H), 4.76 (d, J = 8.9 Hz, 1H), 4.55 (d, J = 7.8 Hz, 1H), 4.24 (q, J = 6.6 Hz, 1H), 4.01 (dd, J_1= 1.9 Hz, J_2 = 12.2 Hz, 1H), 3.91 (d, J = 3.4 Hz, 1H), 3.89 (dd, J_1= 3.4 Hz, J_2 = 9.5 Hz, 1H), 3.85−3.70 (m, 8 H), 3.69 (dd, J_1= 7.8 Hz, J_2 = 9.4 Hz, 1H), 3.64 (dd, J_1= 9.0 Hz, J_2 = 9.3 Hz, 1H), 3.58 (ddd, J_1= 1.8 Hz, J_2 = 5.3 Hz, J_2 = 9.9 Hz, 1H), 3.35 (dd, J_1= 8.9 Hz, J_2 = 9.1 Hz, 1H), 1.25 (d, J = 6.6 Hz, 3H); ^{13}C NMR (125 MHz, D_2O) δ 100.2, 99.4, 90.0, 77.2, 76.3, 75.3, 75.2, 74.3, 73.6, 72.6, 71.7, 69.6, 69.1, 68.2, 66.9, 61.1, 60.0, 15.3.

DISCUSSION

WbsJ, the α1,2-FucT from *E. coli* O128:B12, was classified into the glycosyltransferase family 11 (GT11) based

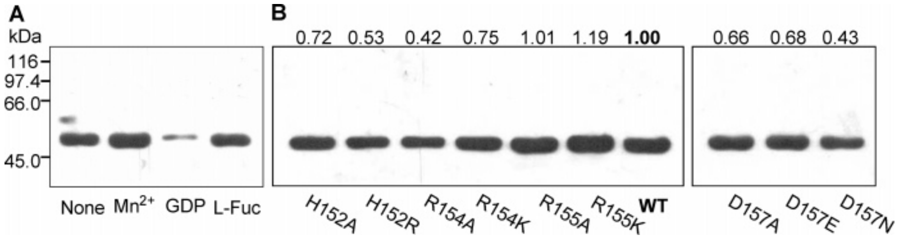

FIGURE 8: Binding of GST-WbsJ and mutants to GDP-beads. GDP-beads were incubated with purified GST-WbsJ or mutants in the binding buffer. The bound enzyme was detected by Western blot using anti-GST antibody and anti-mouse IgG-HRP. (A) Western blot of wild-type GST-WbsJ binding to GDP-beads in the absence (labeled as none) or presence of 10 mM Mn^{2+}, 25 mM GDP or 25 mM L-fucose (L-Fuc). (B) Western blot analysis of the binding of GST-WbsJ mutants to GDP-beads in the absence of Mn^{2+} compared with the wild type. The relative GDP binding activities with comparison of the wild type (as 1.00) are shown on top of each lane. WT: wild type.

on sequence similarities. All the members of GT11 functionally determined thus far are α1,2-FucTs, including FUT1 and FUT2 from humans, as well as *Hp fucT2* from *H. pylori*. WbsJ showed a low level of sequence similarity to its counterparts in prokaryotes and eukaryotes (29% to *Hp fucT2* and 22% to human FUT2). Alignment of mammalian and bacterial α1,2-FucT sequences from GenBank showed even lower similarity among different strains. However, several conserved motifs were identified, indicating the possible location of the catalytic domain. Sequence analysis using MEME (http://meme.nbcr.net/) revealed that, apart from the three common motifs (motif I, II, III) (*25*), motif IV was also found among the mammalian and bacterial α1,2-FucTs at the N-terminus (Figure 6). The function of motif IV is not clear; it likely plays an important structural role. The conserved motifs I, II and III are also shared by α1,6-FucTs and *O*-FucTs, suggesting that they originated from a common ancestor gene or from common ancestor gene duplication (*4*). However, the same motifs are not present in α1,3-fucosyltransferases (*25*). The conserved regions suggest that α1,2-FucTs and α1,6-FucTs may share common structural and catalytic features (*5*). A recent crystal structure of human α1,6-FucT (FUT8) revealed that the three highly conserved motifs are located adjacent to one another and within the Rossmann fold of FUT8 (*31*). These results strongly suggest that these three motifs are key components in the catalytic center, involved in binding GDP-fucose and transferring fucose (*31*).

The Roles of Conserved Residues within Motif I in α1,2-FucT Activity. A single tripeptide sequence DXD motif was found to be conserved in 13 families of glycosyltransferases (*24*). Crystal structures indicate that the DXD motif participates in coordination of a divalent metal ion required for the binding of the nucleotide sugar (*42*). Derivatives of the DXD motif such as XDD and EXD motif were found in human β1,3-glucuronosyltransferase (*43*) and yeast α1,2-mannosyltransferase (*44*), respectively. For glycosyltransferases that are metal ion independent, basic residues were shown to make direct contacts with the pyrophosphate moiety of the nucleotide donor (*45*, *46*). A recently published crystal structure of α1,3-FucT of *H. pylori* further illustrated this binding mode in glycosyltransferases that lack a DXD motif. The critical positively charged residue Arg^{195} forms two H-bonds with the α-phosphate and β-phosphate (*28*).

The results in this study led us to propose that the highly conserved basic-residue-rich motif HxRRxD shared by α1,2-FucTs and α1,6-FucTs likely is in direct contact with the donor GDP-fucose. Mutagenesis followed by kinetic analysis of the mutants of this motif revealed that the R^{154} (universally conserved in α1,2-FucTs and α1,6-FucTs) may directly contact the phosphate group of GDP-fucose. Decreased binding ability to GDP-bead also demonstrates the interaction between R^{154} and GDP moiety. The kinetic data of mutants R155A and R155K are in agreement with that of human α1,6-FucT at equivalent R^{366} (*41*). However, no impaired binding to GDP-beads was observed for mutants R155A and R155K compared with the wild type. GDP-bead binding assay may not be a good method to characterize the dynamic binding interaction between fucosyltransferase and substrate. Many factors could affect the binding assay, such as the ratio of bead and protein and/or the binding time. The mutations at R^{154} and R^{155} might not only influence the donor substrate binding, but also interfere with the acceptor binding, leading to a higher K_m value for the acceptor. In contrast to human α1,6-FucT, H^{152} of α1,2-FucT (corresponding to H^{363} of human α1,6-FucT) also plays an important role in catalysis, illustrated by the increased K_m values of H^{152} mutants for both donor and acceptor substrates as well as the decreased binding affinity to GDP-beads. The differences in activity between α1,2-FucT and human α1,6-FucT at the residue H^{152} and R^{154} may be explained by the existence of two different enzyme mechanisms.

Consistent with the mutagenesis results of FUT8, D^{157} is critical for enzyme function (*31*). Mutations at D^{157} drastically decrease the enzyme activity, indicating that D^{157} is a very important residue. Crystal structure of human α1,6-FucT indicates that the equivalent residue D^{368} is located in disordered flexible loop, suggesting its important role in catalytic mechanism. In conclusion, the highly conserved motif HxRRxD is important for binding to GDP-fucose. Within this motif, residue R^{154} and D^{157} play critical roles in binding to GDP-fucose and catalytic functions.

Acceptor Specificity of WbsJ and Comparison with Other α1,2-FucTs. The catalytic properties of the two α1,2-FucTs in humans are different (*8*, *47*, *48*). FUT1 transfers a fucose equally well to both type 1 and type 2 precursors (Galβ1,3GlcNAc, Galβ1,4GlcNAc) and less well to the type 3/4 precursor (Galβ1,3GalNAc). FUT2, in contrast, shows a remarkable preference for the type 1 and type 3/4 precursors (*8*). Human gastric pathogen *H. pylori* α1,2-FucT prefers Lewis X [Galβ1,4(Fucα1,3)GlcNAcβ] over LacNAc (Galβ1,4GlcNAcβ) as a substrate. *H. pylori* α1,2-FucT also acts on type 1 and Lewis a [Galβ1,3(Fucα1,4)GlcNAcβ] to synthesize H-type 1 and Lewis b epitopes (*17*).

WbsJ showed very broad acceptor specificity. WbsJ prefers type 3 (Galβ1,3GalNAcα, blood T antigen) and type 5 (Galβ1,4Glc, lactose) precursors to synthesize H-type 3 (Fucα1,2Galβ1,3GalNAcα) and H-type 5 (Fucα1,2Galβ1,-

4Glc) antigens, respectively. WbsJ also acts very well on lactulose (Galβ1,4Fru) and Galβ1,4Man. In addition, WbsJ showed moderate activity with Gal or Galβ-*O*-Me as acceptors. Successful milligram-scale syntheses of fucosylated di- and trisaccharides in this work demonstrate the potential of WbsJ for application in the synthesis of H antigen Fucα1,2Galβ-R.

Broad acceptor specificity of WbsJ indicates a relaxed binding pocket for acceptor substrates. It is proposed that glycosyltransferases have two domains, one for nucleotide binding and the other for acceptor binding, connected by an interface cleft where the catalytic center is located (*49*). We propose that the hypervariable region of bacterial α1,2-FucT might be responsible for determining the acceptor specificity. Further experiments such as domain swapping between *E. coli* O128:B12 and other α1,2-FucTs might help elucidate the critical residues for acceptor specificity.

Secondary Structure Prediction of α*1,2-FucT from E. coli O128:B12.* The secondary structure of WbsJ was predicted by PSA (protein sequence analysis) and PSIPRED (position-specific iterated protein structure prediction) (*50*). The result (see the Supporting Information) suggested that WbsJ is an α/β fold protein with >85% probability. There is a three-layer $\beta/\alpha/\beta$ sandwich Rossmann-fold topology at the C-terminal domain of WbsJ. Moreover, the highly conserved basic residues of motif I are located at the random-coil region. The crystal structures of a number of glycosyltransferases show that a flexible loop region is crucial for catalysis and located in the vicinity of nucleotide−sugar binding site (*33*). The Rossmann fold is a well-known nucleotide or nucleotide−sugar binding domain. The crystal structure of the α1,3-FucT/GDP-fucose complex shows that the C-terminal Rossmann fold is the binding site of GDP-fucose (*28*). Additionally, the crystal structure of human α1,6-FucT (FUT8) also reveals that a Rossmann fold containing flexible loop is located at the C-terminal domain, a feature which possibly forms the GDP-fucose binding domain (*31*). The Rossmann fold in FUT8 covers the conserved motif I, II and III shared by α1,2-FucTs, α1,6-FucTs and *O*-FucTs. The secondary structure of α1,2-FucT WbsJ is similar to α1,6-FucT at the C-terminal domain (residue 130−250), but not at the N-terminal domain. This observation suggests that the N-terminus may contain the acceptor-binding domain and determine the substrate specificity. Like α1,6-FucTs, α1,2-FucTs could belong to a superfamily different from the GT-A fold but similar to the GT-B fold (*31*). Efforts to further investigate the WbsJ mechanism by crystallography are ongoing.

SUPPORTING INFORMATION AVAILABLE

MS spectra and NMR spectra of Fucα1,2Galβ-*O*-Me and Fucα1,2Galβ1,4Glcβ-N_3 synthesized using GST-WbsJ. Secondary structure prediction of WbsJ. This material is available free of charge via the Internet at http://pubs.acs.org.

REFERENCES

1. Oriol, R., Samuelsson, B. E., and Messeter, L. (1990) ABO antibodies−serological behaviour and immuno-chemical characterization, *J. Immunogenet. 17*, 279−299.
2. Becker, D. J., and Lowe, J. B. (2003) Fucose: biosynthesis and biological function in mammals, *Glycobiology 13*, 41R-53R.
3. Ma, B., Simala-Grant, J. L., and Taylor, D. E. (2006) Fucosylation in prokaryotes and eukaryotes, *Glycobiology 16*, 158R-184R.
4. Martinez-Duncker, I., Mollicone, R., Candelier, J. J., Breton, C., and Oriol, R. (2003) A new superfamily of protein-*O*-fucosyltransferases, α2-fucosyltransferases, and α6-fucosyltransferases: phylogeny and identification of conserved peptide motifs, *Glycobiology 13*, 1C-5C.
5. Chazalet, V., Uehara, K., Geremia, R. A., and Breton, C. (2001) Identification of essential amino acids in the *Azorhizobium caulinodans* fucosyltransferase NodZ, *J. Bacteriol. 183*, 7067−7075.
6. Larsen, R. D., Ernst, L. K., Nair, R. P., and Lowe, J. B. (1990) Molecular cloning, sequence, and expression of a human GDP-L-fucose:β-D-galactoside 2-α-L-fucosyltransferase cDNA that can form the H blood group antigen, *Proc. Natl. Acad. Sci. U.S.A. 87*, 6674−6678.
7. Sarnesto, A., Kohlin, T., Thurin, J., and Blaszczyk-Thurin, M. (1990) Purification of H gene-encoded β-galactoside α1,2-fucosyltransferase from human serum, *J. Biol. Chem. 265*, 15067−15075.
8. Sarnesto, A., Kohlin, T., Hindsgaul, O., Thurin, J., and Blaszczyk-Thurin, M. (1992) Purification of the secretor-type β-galactoside α1,2-fucosyltransferase from human serum, *J. Biol. Chem. 267*, 2737−2744.
9. Kelly, R. J., Rouquier, S., Giorgi, D., Lennon, G. G., and Lowe, J. B. (1995) Sequence and expression of a candidate for the human secretor blood group α(1,2)fucosyltransferase gene (FUT2). Homozygosity for an enzyme-inactivating nonsense mutation commonly correlates with the non-secretor phenotype, *J. Biol. Chem. 270*, 4640−4649.
10. Hitoshi, S., Kusunoki, S., Kanazawa, I., and Tsuji, S. (1995) Molecular cloning and expression of two types of rabbit β-galactoside α1,2-fucosyltransferase, *J. Biol. Chem. 270*, 8844−8850.
11. Domino, S. E., Zhang, L., and Lowe, J. B. (2001) Molecular cloning, genomic mapping, and expression of two secretor blood group α(1,2)fucosyltransferase genes differentially regulated in mouse uterine epithelium and gastrointestinal tract, *J. Biol. Chem. 276*, 23748−23756.
12. DeBose-Boyd, R. A., Nyame, A. K., and Cummings, R. D. (1998) Molecular cloning and characterization of an α1,3 -fucosyltransferase, CEFT-1, from *Caenorhabditis elegans*, *Glycobiology 8*, 905−917.
13. Perrin, R. M., DeRocher, A. E., Bar-Peled, M., Zeng, W., Norambuena, L., Orellana, A., Raikhel, N. V., and Keegstra, K. (1999) Xyloglucan fucosyltransferase, an enzyme involved in plant cell wall biosynthesis, *Science 284*, 1976−1979.
14. Oriol, R. (1990) Genetic control of the fucosylation of ABH precursor chains. Evidence for new epistatic interactions in different cells and tissues, *J. Immunogenet. 17*, 235−245.
15. Yamamoto, F., Clausen, H., White, T., Marken, J., and Hakomori, S. (1990) Molecular genetic basis of the histo-blood group ABO system, *Nature 345*, 229−233.
16. Bureau, V., Marionneau, S., Cailleau-Thomas, A., Le Moullac-Vaidye, B., Liehr, T., and Le Pendu, J. (2001) Comparison of the three rat GDP-L-fucose:β-D-galactoside 2-α-L-fucosyltransferases FTA, FTB and FTC, *Eur. J. Biochem. 268*, 1006−1019.
17. Wang, G., Boulton, P. G., Chan, N. W., Palcic, M. M., Taylor, D. E. (1999) Novel *Helicobacter pylori* α1,2-fucosyltransferase, a key enzyme in the synthesis of Lewis antigens, *Microbiology 145* (Part 11), 3245−3253.
18. Sengupta, P., Bhattacharyya, T., Shashkov, A. S., Kochanowski, H., and Basu, S. (1995) Structure of the O-specific side chain of the *Escherichia coli* O128 lipopolysaccharide, *Carbohydr. Res. 277*, 283−290.
19. Lerouge, I., and Vanderleyden, J. (2002) O-antigen structural variation: mechanisms and possible roles in animal/plant-microbe interactions, *FEMS Microbiol. Rev. 26*, 17−47.
20. Rietschel, E. T., Brade, H., Holst, O., Brade, L., Muller-Loennies, S., Mamat, U., Zahringer, U., Beckmann, F., Seydel, U., Brandenburg, K., Ulmer, A. J., Mattern, T., Heine, H., Schletter, J., Loppnow, H., Schonbeck, U., Flad, H. D., Hauschildt, S., Schade, U. F., Di, Padova, F., Kusumoto, S., and Schumann, R. R. (1996) Bacterial endotoxin: Chemical constitution, biological recognition, host response, and immunological detoxification, *Curr. Top. Microbiol. Immunol. 216*, 39−81.
21. Moran, A. P., Prendergast, M. M., and Appelmelk, B. J. (1996) Molecular mimicry of host structures by bacterial lipopolysaccharides and its contribution to disease, *FEMS Immunol. Med. Microbiol. 16*, 105−115.

22. Sengupta, P., Bhattacharyya, T., Majumder, M., and Chatterjee, B. P. (2000) Determination of the immunodominant part in the O-antigenic polysaccharide from *Escherichia coli* O128 by ELISA-inhibition study, *FEMS Immunol. Med. Microbiol. 28*, 133−137.
23. Shao, J., Li, M., Jia, Q., Lu, Y., and Wang, P. G. (2003) Sequence of *Escherichia coli* O128 antigen biosynthesis cluster and functional identification of an α-1,2-fucosyltransferase, *FEBS Lett. 553*, 99−103.
24. Breton, C., Oriol, R., and Imberty, A. (1998) Conserved structural features in eukaryotic and prokaryotic fucosyltransferases, *Glycobiology 8*, 87−94.
25. Oriol, R., Mollicone, R., Cailleau, A., Balanzino, L., and Breton, C. (1999) Divergent evolution of fucosyltransferase genes from vertebrates, invertebrates, and bacteria, *Glycobiology 9*, 323−334.
26. Ma, B., Wang, G., Palcic, M. M., Hazes, B., and Taylor, D. E. (2003) C-terminal amino acids of *Helicobacter pylori* α1,3/4 fucosyltransferases determine type I and type II transfer, *J. Biol. Chem. 278*, 21893−21900.
27. Ma, B., Audette, G. F., Lin, S., Palcic, M. M., Hazes, B., and Taylor, D. E. (2006) Purification, kinetic characterization, and mapping of the minimal catalytic domain and the key polar groups of *Helicobacter pylori* α-(1,3/1,4)-fucosyltransferases, *J. Biol. Chem. 281*, 6385−6394.
28. Sun, H. Y., Lin, S. W., Ko, T. P., Pan, J. F., Liu, C. L., Lin, C. N., Wang, A. H., and Lin, C. H. (2007) Structure and mechanism of *Helicobacter pylori* fucosyltransferase. A basis for lipopolysaccharide variation and inhibitor design, *J. Biol. Chem. 282*, 9973−9982.
29. Uozumi, N., Yanagidani, S., Miyoshi, E., Ihara, Y., Sakuma, T., Gao, C. X., Teshima, T., Fujii, S., Shiba, T., and Taniguchi, N. (1996) Purification and cDNA cloning of porcine brain GDP-L-Fuc:N-acetyl-β-D-glucosaminide α1,6-fucosyltransferase, *J. Biol. Chem. 271*, 27810−27817.
30. Yamaguchi, Y., Fujii, J., Inoue, S., Uozumi, N., Yanagidani, S., Ikeda, Y., Egashira, M., Miyoshi, O., Niikawa, N., and Taniguchi, N. (1999) Mapping of the α-1,6-fucosyltransferase gene, FUT8, to human chromosome 14q24.3, *Cytogenet. Cell Genet. 84*, 58−60.
31. Ihara, H., Ikeda, Y., Toma, S., Wang, X., Suzuki, T., Gu, J., Miyoshi, E., Tsukihara, T., Honke, K., Matsumoto, A., Nakagawa, A., and Taniguchi, N. (2007) Crystal structure of mammalian α1,6-fucosyltransferase, FUT8, *Glycobiology 17*, 455−466.
32. Quiros, L. M., Carbajo, R. J., Brana, A. F., and Salas, J. A. (2000) Glycosylation of macrolide antibiotics. Purification and kinetic studies of a macrolide glycosyltransferase from Streptomyces antibioticus, *J. Biol. Chem. 275*, 11713−11720.
33. Qasba, P. K., Ramakrishnan, B., and Boeggeman, E. (2005) Substrate-induced conformational changes in glycosyltransferases, *Trends Biochem. Sci. 30*, 53−62.
34. Hu, Y., Chen, L., Ha, S., Gross, B., Falcone, B., Walker, D., Mokhtarzadeh, M., and Walker, S. (2003) Crystal structure of the MurG:UDP-GlcNAc complex reveals common structural principles of a superfamily of glycosyltransferases, *Proc. Natl. Acad. Sci. U.S.A. 100*, 845−849.
35. Mulichak, A. M., Losey, H. C., Walsh, C. T., and Garavito, R. M. (2001) Structure of the UDP-glucosyltransferase GtfB that modifies the heptapeptide aglycone in the biosynthesis of vancomycin group antibiotics, *Structure 9*, 547−557.
36. Beyer, T. A., and Hill, R. L. (1980) Enzymatic properties of the β-galactoside α 1 leads to 2 fucosyltransferase from porcine submaxillary gland, *J. Biol. Chem. 255*, 5373−5379.
37. Ihara, H., Ikeda, Y., and Taniguchi, N. (2006) Reaction mechanism and substrate specificity for nucleotide sugar of mammalian α1,6-fucosyltransferase − a large-scale preparation and characterization of recombinant human FUT8, *Glycobiology 16*, 333−342.
38. Wong, C.-H., Ruo Wang, R., and Ichikawa, Y. (1992) Regeneration of sugar nucleotide for enzymic oligosaccharide synthesis: use of Gal-1-phosphate uridyltransferase in the regeneration of UDP-galactose, UDP-2-deoxygalactose, and UDP-galactosamine, *J. Org. Chem. 57*, 4343−4344.
39. Faik, A., Bar-Peled, M., DeRocher, A. E., Zeng, W., Perrin, R. M., Wilkerson, C., Raikhel, N. V., and Keegstra, K. (2000) Biochemical characterization and molecular cloning of an α-1,2-fucosyltransferase that catalyzes the last step of cell wall xyloglucan biosynthesis in pea, *J. Biol. Chem. 275*, 15082−15089.
40. Miyashiro, M., Furuya, S., and Sugita, T. (2004) Development of a sensitive separation and quantification method for sialyl Lewis X and Lewis X involving anion-exchange chromatography: biochemical characterization of α1−3 fucosyltransferase-VII, *J. Biochem. (Tokyo) 136*, 723−731.
41. Takahashi, T., Ikeda, Y., Tateishi, A., Yamaguchi, Y., Ishikawa, M., and Taniguchi, N. (2000) A sequence motif involved in the donor substrate binding by α1,6-fucosyltransferase: the role of the conserved arginine residues, *Glycobiology 10*, 503−510.
42. Unligil, U. M., and Rini, J. M. (2000) Glycosyltransferase structure and mechanism, *Curr. Opin. Struct. Biol. 10*, 510−517.
43. Gulberti, S., Fournel-Gigleux, S., Mulliert, G., Aubry, A., Netter, P., Magdalou, J., and Ouzzine, M. (2003) The functional glycosyltransferase signature sequence of the human β1,3-glucuronosyltransferase is a XDD motif, *J. Biol. Chem. 278*, 32219−32226.
44. Lobsanov, Y. D., Romero, P. A., Sleno, B., Yu, B., Yip, P., Herscovics, A., and Howell, P. L. (2004) Structure of Kre2p/Mnt1p: a yeast α1,2-mannosyltransferase involved in mannoprotein biosynthesis, *J. Biol. Chem. 279*, 17921−17931.
45. Ha, S., Walker, D., Shi, Y., and Walker, S. (2000) The 1.9 Å crystal structure of *Escherichia coli* MurG, a membrane-associated glycosyltransferase involved in peptidoglycan biosynthesis, *Protein Sci. 9*, 1045−1052.
46. Vrielink, A., Ruger, W., Driessen, H. P., and Freemont, P. S. (1994) Crystal structure of the DNA modifying enzyme β-glucosyltransferase in the presence and absence of the substrate uridine diphosphoglucose, *EMBO J. 13*, 3413−3422.
47. Masutani, H., and Kimura, H. (1995) Purification and characterization of secretory-type GDP-L-fucose:β-D-galactoside 2-α-L-fucosyltransferase from human gastric mucosa, *J. Biochem. (Tokyo) 118*, 541−545.
48. Le Pendu, J., Cartron, J. P., Lemieux, R. U., and Oriol, R. (1985) The presence of at least two different H-blood-group-related β-D-gal α-2-L-fucosyltransferases in human serum and the genetics of blood group H substances, *Am. J. Hum. Genet. 37*, 749−760.
49. Hoffmeister, D., Ichinose, K., and Bechthold, A. (2001) Two sequence elements of glycosyltransferases involved in urdamycin biosynthesis are responsible for substrate specificity and enzymatic activity, *Chem. Biol. 8*, 557−567.
50. McGuffin, L. J., Bryson, K., and Jones, D. T. (2000) The PSIPRED protein structure prediction server, *Bioinformatics 16*, 404−405.

BI701345V